

W-37

ARR Mar. 1943

NATIONAL ADVISORY COMMITTEE FOR AERONAUTICS

WARTIME REPORT

ORIGINALLY ISSUED

March 1943 as
Advance Restricted Report

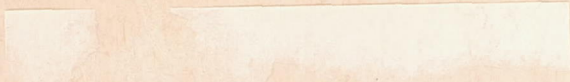
A METHOD FOR STUDYING PISTON FRICTION

By J. E. Forbes and E. S. Taylor
Massachusetts Institute of Technology



WASHINGTON

NACA WARTIME REPORTS are reprints of papers originally issued to provide rapid distribution of advance research results to an authorized group requiring them for the war effort. They were previously held under a security status but are now unclassified. Some of these reports were not technically edited. All have been reproduced without change in order to expedite general distribution.



NATIONAL ADVISORY COMMITTEE FOR AERONAUTICS

ADVANCE RESTRICTED REPORT

A METHOD FOR STUDYING PISTON FRICTION

By J. E. Forbes and E. S. Taylor

INTRODUCTION

The purpose of this investigation was to develop a method for determining directly the friction force between the piston and cylinder of an internal combustion engine.

The method consists in elastically mounting the cylinder barrel so that it can have a small motion parallel to its axis, and providing suitable means for recording its instantaneous displacement.

DESCRIPTION OF APPARATUS

Cylinder and Cylinder Head

The cylinder barrel in the form of a light sleeve (see fig. 1(1)) is clamped on the inner circumferences of two annular steel diaphragms (2). The outer circumferential edges of the diaphragms are clamped to a cylindrical water jacket (3) by means of a steel plate (4) at one end and the cylinder head (5) at the other end.

The cylinder head closes the combustion chamber with a piston-shaped section. This section is machined so as to form a labyrinth seal (6) to the combustion gases, and yet not restrain the cylinder-sleeve motion. The labyrinth section of the head is lead-plated so as to insure a close fit with a minimum of friction.

Two spark-plug wells (7) and a well containing an optical lever (8) are sealed off from the jacket cooling water by means of flexible neoprene seals (9). These seals exert no appreciable constraint on the cylinder motion.

Vent holes (10) drilled in the side of the cylinder head into the space above the diaphragm take care of gas leakage through the labyrinth, and assure atmospheric pressure on the upper diaphragm.

Reduction of gas leakage through the labyrinth is provided by a duct (11) leading through the top of the cylinder head to the center of the labyrinth. Lubricating oil similar to that used in the engine is pumped by means of an externally driven oil pump through this duct at a pressure of about 50 pounds per square inch. The oil passes through the labyrinth into the space (12) above the upper diaphragm and then out through the vent holes to the oil-pump reservoir. Under favorable running conditions only a small percentage of this sealing oil flows into the combustion chamber.

Cylinder-Displacement Measuring System

The displacement of the cylinder sleeve is recorded photographically on motion-picture film by means of an optical lever and strip camera (reference 1). (See figs. 2, 3, 4, and 5.) A film speed of 25 inches per second was used throughout the tests. The magnification of the cylinder-sleeve displacement, by means of the optical system, was 70.6. (See fig. 6.) Calibration curves of the static performance of the recording system at two different water-jacket temperatures are shown in figure 7. These and similar curves were obtained by statically loading the assembled cylinder when the regular cylinder head had been replaced by a "dummy head." This dummy head was a steel ring which clamped the outer edge of the upper diaphragm firmly in its place. A steel plug fitting into the exposed end of the cylinder served as a loading platform. During these tests the piston was removed from the cylinder. Actual sleeve displacement due to static load was measured by a sensitive dial gage. Strips of film were run through the camera with and without each static load. These records gave the net film-trace displacements corresponding to the dial-gage readings or loads.

The curves of figure 7 show that the stiffness of the diaphragms varies with water-jacket temperature. A curve of diaphragm stiffness covering the temperature-operating range of the tests presented in this report is shown in figure 8.

Pistons

The aluminum-alloy piston with its five cast-iron piston rings shown in figure 9 was used throughout the tests pertaining to the effects of speed, load, and viscosity. The cast-iron piston, also illustrated in figure 9, was used only in the "running-in" test.

Engine

The complete cylinder assembly was mounted on a standard CFR crankcase. A shorter connecting rod (length = 8.00 in.) than standard with the CFR was used, giving a crank-throw to connecting-rod-length ratio of 0.281. The bore and stroke were standard 3.25 by 4.5 inches. The compression ratio was 5.05.

Lubrication System

The standard CFR oil pump was removed, and a motor-driven oil pump substituted to circulate the engine-lubricating oil. Oil temperature was controlled by means of a heat exchanger through which either steam or water or both could be circulated. Oil temperature was measured in the oil pump by means of a vapor-pressure thermometer.

Cooling System

Cooling was accomplished by a closed system consisting of a 7-gallon tank, a separately motor-driven centrifugal pump, a heat exchanger, and the cylinder water jacket. The heat exchanger was similar to that used on the lubricating system. Distilled water containing a rust inhibitor was used in this closed system so as to reduce rusting of the exposed areas of the diaphragms and the cylinder sleeve. A mercury-in-glass thermometer inserted in the upper end of the water jacket was used to measure the jacket-water temperature. Cold tap water was circulated through the cylinder head. The temperature of this water was measured by a mercury-in-glass thermometer located at the cooling-water outlet of the head.

Inlet System

Fuel-air mixture was supplied to the engine from a vaporizing tank (reference 2). The inlet air passed through a fuel-mixing orifice inserted in the vaporizing tank. The air flow to the tank was controlled by a throttling valve. Fuel was measured by means of a calibrated rotameter. Mixture temperature was measured by a mercury-in-glass thermometer placed in the inlet pipe. Vaporizing tank pressure was measured by a mercury manometer.

Engine Instruments

Engine speed was controlled by a combination of a conventional tachometer and a stroboscopic light running directly from the 60-cycle supply that illuminated painted strips on the flywheel (reference 2). An electric dynamometer was used. Pressure against crank-angle diagrams was obtained from the standard M.I.T. balanced-pressure indicator using an M.I.T. diaphragm pressure unit (references 3 and 4).

RESULTS AND DISCUSSION

Reduction of Data

A typical photographic record of the sleeve displacement is shown in figure 10, which is a firing record taken at 2035 rpm. The heavy vertical lines are the top-center locating lines produced by a flashing neon light. (See fig. 2.) This neon light flashes simultaneously with the ignition spark. The position of the neon light in the camera is such as to mark the film 0.26 inch from the record trace and thus locate the ignition crank angle on the time axis. θ degrees of crank angle along the film axis, with a film speed of 25 inches per second and an engine speed N rpm, correspond to a length L on this axis equal to $4.17 \theta/N$ inch. Hence top center on the film trace is located a distance $(0.26 - L)$ inch along the time axis to the left of the center of the neon lamp flash.

The dim diffuse line appearing parallel to the time axis in most of the records is a reflected trace of the light source from the front surface of the lens. The records in general show

essentially three types of excitation of the sleeve, that is, over-all displacements corresponding to the piston strokes, a rather prominent excitation occurring during the firing stroke, and finally some high-frequency excitation of comparatively low amplitude. Photographic records of the natural frequency of vibration of the cylinder sleeve with engine completely assembled, also with piston removed, and the dummy head in place of the regular cylinder head are shown in figure 11. These records together with calculations made of the natural frequency of vibration of the sleeve from its known stiffness and weight show that the prominent excitation of the sleeve in all the records corresponds to its natural frequency. The origin of the high-frequency excitation is not conclusively known.

Owing to the fact that the diaphragm system was sensitive to temperature changes, there appeared to be no satisfactory method of recording on the films a "zero line," that is, a line indicating the equilibrium position of the cylinder sleeve when no force was acting on it. Establishment of the probable zero line was accomplished in the following manner: An enlarged trace of the photographic record was made in an enlarging camera. A straight line parallel to the film motion is then so drawn as to intersect the enlarged record at four equally spaced points during the time interval of each cycle. This line is then taken as the zero line from which all displacements on the enlarged record are measured. From the magnification of the enlargement and the stiffness calibration curve (fig. 8), the displacements are readily converted into equivalent piston-friction forces on the assumption that the inertia and damping forces are negligible compared to the diaphragm force.

While the location of the true zero line may be somewhat in doubt, and thus produce errors in the true instantaneous piston-friction forces, it is significant that the piston-friction work, as obtained from the work loops, is not subject to any error made in locating this line. The work loops are the basis for computing piston-friction mean-effective pressures, and the piston-friction horsepowers herein reported, and hence these values are not subject to zero-line location errors.

The effects of speed upon piston friction were first measured. Both motoring and firing runs were made over a speed range of 1000 to 2500 rpm at full-throttle setting. The mixture ratio was set in all cases at best power. Spark advance was kept constant at 22° . Cylinder-sleeve cooling-water temperature and oil temperature were each kept constant at 180° F. Inlet-mixture

temperature was maintained constant at 140° F, and cylinder-head cooling-water temperature at 50° F. A low cylinder-head cooling-water temperature was maintained so as to minimize the possibility of melting the lead plating on the labyrinth section of the cylinder head. The lubricating oil used in these runs was SAE 40, having a viscosity of 23.9 centipoise at 180° F.

A series of these speed records is shown in figure 12.

Piston-friction work cycles obtained from some of these records are shown in figure 13. The total area enclosed by the two loops represents the piston-friction work per cycle.

The solid-line loops are for the expansion-exhaust strokes while the dashed lines are for the inlet-compression strokes. This scheme of differentiating the two phases applies to all piston-friction work loops presented in this report.

Piston-friction mean-effective pressures computed from these work diagrams are plotted against speed in figure 14.

Firing piston-friction mean-effective pressures over the tested speed range vary from 18 to 46 percent higher than those for motoring. This difference in the relative magnitude, shown by the piston-friction mean-effective-pressure curves in figure 14, probably accounts to a large extent for the similar divergence depicted in the two indicated mean-effective-pressure curves. The lower indicated mean-effective-pressure curve was obtained by adding the brake-motoring and brake-firing curves, whereas the other indicator curve was obtained by use of the M.I.T. high-speed engine indicator (references 3 and 4). Firing piston-friction mean-effective pressure increases linearly with speed and is about 45 percent greater at 2500 rpm than at 1000 rpm.

A considerable number of check runs were made on these speed records. Comparison of the check records with those of the original runs showed very good reproducibility both in magnitude and structure.

Effect of Load

The effect of load on piston friction at two different speeds is shown in figure 15, and the corresponding work loops are shown in figure 16. The variation of piston-friction mean-effective pressure with indicated mean-effective pressure for

the two different speeds is shown in figure 17. The engine was run at the same temperatures and with the same quality oil (SAE 40) as in the speed runs. Indicated mean-effective pressures were derived from indicator diagrams obtained with the M.I.T. high-speed engine indicator (references 3 and 4).

At 1500 rpm a change of 1 pound per square inch indicated mean-effective pressure produces a change of 0.033 pound per square inch in piston-friction mean-effective pressure, while at 2500 rpm a 1-pound change in indicated mean-effective pressure increases the piston-friction mean-effective pressure 0.028 pound.

The change of piston-friction mean-effective pressure with speed at any particular load is of the same order of magnitude as found in the speed tests.

Effect of Viscosity

Dependence of piston-friction force on oil and cooling-water temperature is shown in figure 18. These records both of motoring and firing runs were taken at a constant speed of 1800 rpm, with SAE 20 oil. The oil and cylinder-water-jacket temperatures were kept equal to each other and varied over a range of about 100° F. Inlet temperature was held constant at 140° F while the head-cooling water was kept at 48° F. Spark advance was 22° and mixture ratio set for best power. Corresponding piston-friction work diagrams are shown in figure 19.

The variation of viscosities with temperature of the two oils used in these tests is shown in figure 20.

Plots of piston-friction mean-effective pressure against oil viscosity at jacket temperature both for motoring and firing are shown in figure 21.

Examination of the firing photographs (fig. 18(b)) shows a rather interesting performance at 133° F where alternate periods of two cycles seem to reproduce themselves. Examination of the piston rings after the runs with SAE 20 oil showed considerable scuffing. No appreciable scuffing of the rings appeared after the runs using SAE 40 oil. The presence of scuffing might account for the erratic behavior of the records and the irregularity of the lower curve in figure 21. The fact that the motoring runs were taken after the firing runs and show an

orderly trend might indicate that the scuffing condition had been reduced by the time these runs were made. Figure 9A shows the condition of the rings after the motoring runs with SAE 20 oil.

A comparison of the piston-friction mean-effective pressures at equal viscosities based on water-jacket temperatures and at the same speeds and loads for the two oils used in these tests is shown in table, both for firing and motoring.

	Oil SAE	rpm	t °F	Centipoise at jacket temperature	Piston fmop lb/sq in.
Motoring	40	1800	180	23.5	5.4
	20	1800	142	23.5	6.3
Firing	40	1800	180	23.5	8.0
	20	1800	142	23.5	5.5

Piston-Friction Horsepower

Piston-friction horsepower is plotted against motoring horsepower and firing-friction horsepower in figure 22. The firing-friction-horsepower curves were obtained by subtracting the firing brake horsepower from the indicated power taken from indicator cards. The curves indicate that for these experiments the motoring piston-friction horsepower amounts to roughly 16 percent of the motoring horsepower, and that the firing piston-friction horsepower is about 26 percent of the motoring horsepower.

It should be noted that motoring and firing-friction horsepower each includes bearing friction and pumping friction in addition to piston friction.

It should be mentioned that the sealing oil which leaks into the combustion chamber from the cylinder-head labyrinth may reduce the piston friction below that which would be obtained with normal lubrication.

Running-In Test

For comparative purposes a new cast-iron piston was substituted for the aluminum-alloy piston. This piston (see fig. 9B) had three piston rings and a skirt much longer than that of the aluminum one. The two pistons gave the same compression ratio.

Records of motoring friction taken with this piston at 900 rpm are shown as a function of running-in time in figure 23. At intervals between these records the motoring speed was occasionally run up to 1000 rpm, and during an early one of these speed increases an unsteady brake load indicated signs of piston seizing. Examination of the piston after these runs were completed showed scoring of the piston (fig. 9B) and pick-up on the cylinder. In spite of the scoring, a rather significant decrease in piston friction with running-in time is indicated by the decreasing amplitudes of the records in figure 23.

CONCLUSIONS

The results must be regarded as of a preliminary nature until more experience with this apparatus has been obtained. It appears safe to conclude, however, that the method has interesting possibilities for research in the field of piston friction. Further work is suggested to include an attempt to compare piston friction alone, measured by motoring, with piston friction obtained by this method, and to explore systematically the effects of differences in piston and ring design.

Sloan Laboratories for Aircraft and Automotive Engines,
Massachusetts Institute of Technology,
Cambridge, Mass.

REFERENCES

1. Bouchard, C. L., Taylor, C. F., and Taylor, E. S.: Variables Affecting Flame Speed in the Otto-Cycle Engine. Jour. SAE, vol. 41, no. 5, Nov. 1937.
2. Taylor, E. S., Leary, W. A., and Diver, J. R.: Effect of Fuel-Air Ratio, Inlet Temperature, and Exhaust Pressure on Detonation. Rep. No. 699, NACA, 1940.
3. Reynolds, Blake, Schechter, Harry, and Taylor, E. S.: The Charging Process in a High-Speed, Single-Cylinder, Four-Stroke Engine. T.N. No. 675, NACA, 1939.
4. Taylor, E. S., and Draper, C. S.: A New High-Speed Engine Indicator. Mech. Eng., vol. 55, no. 3, March 1933, pp. 169-171.

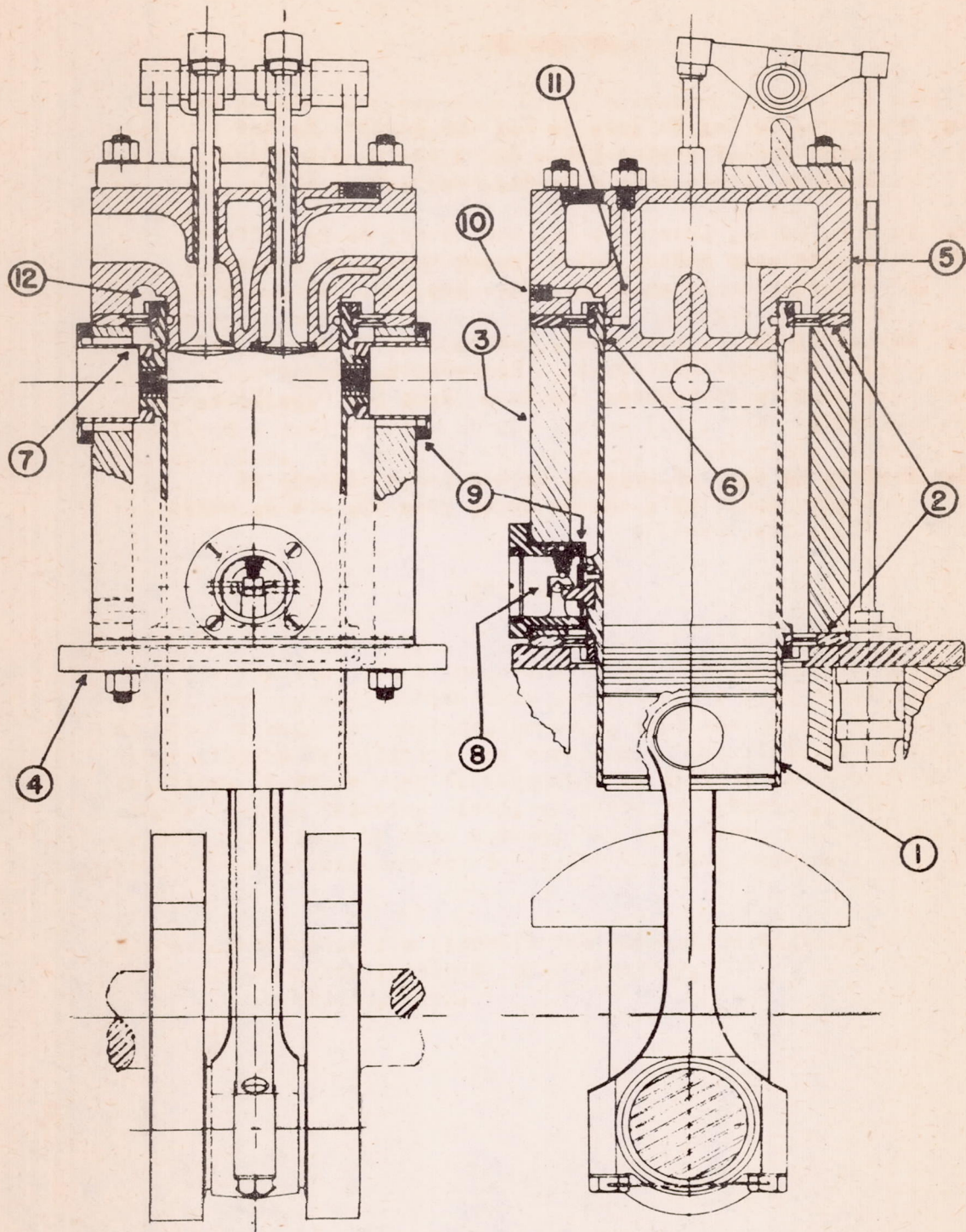


Figure 1.- Assembly drawing of friction engine cylinder.

W-37

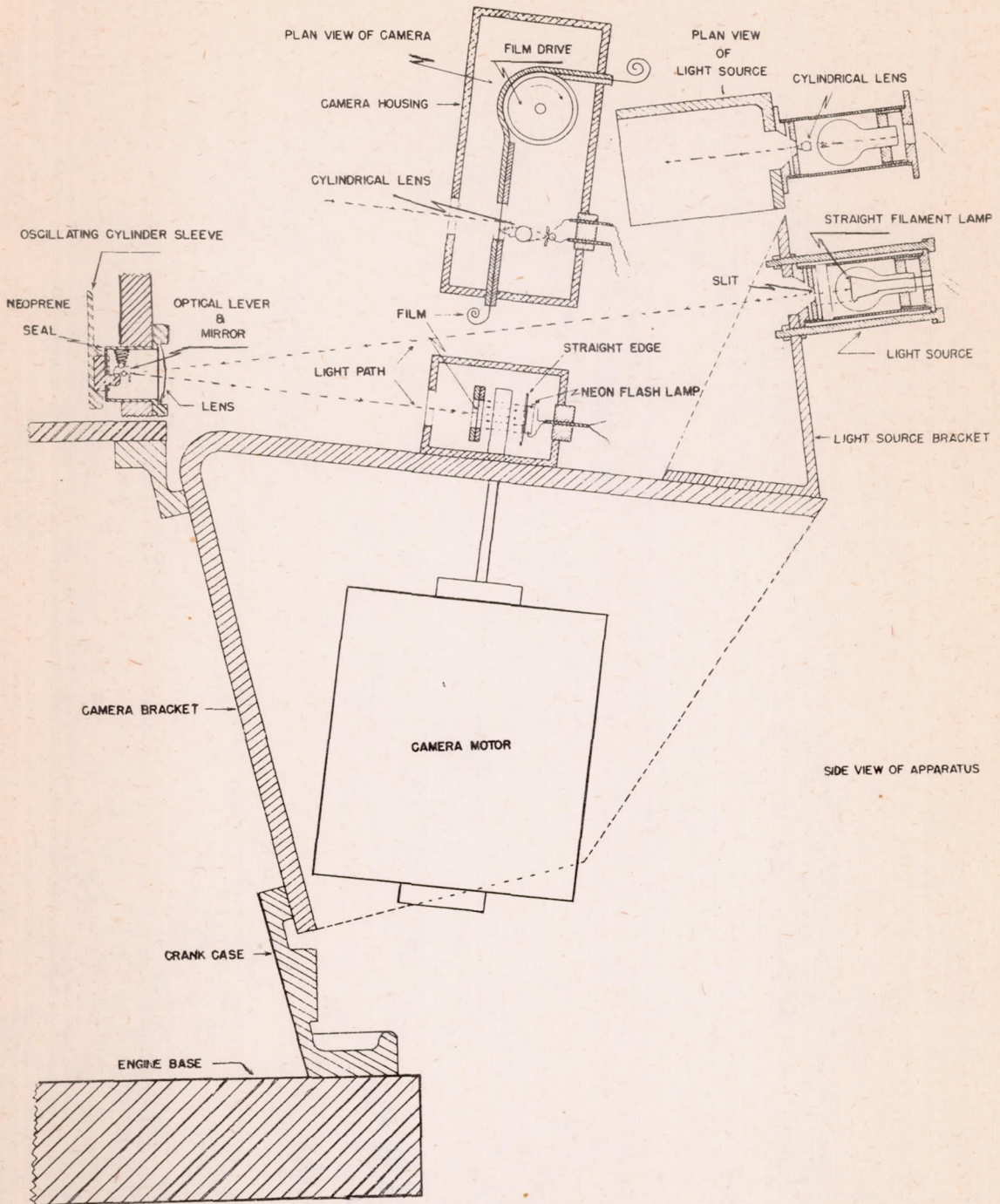


Figure 2.- Details of optical system for recording cylinder sleeve displacements.

W-37

W-37

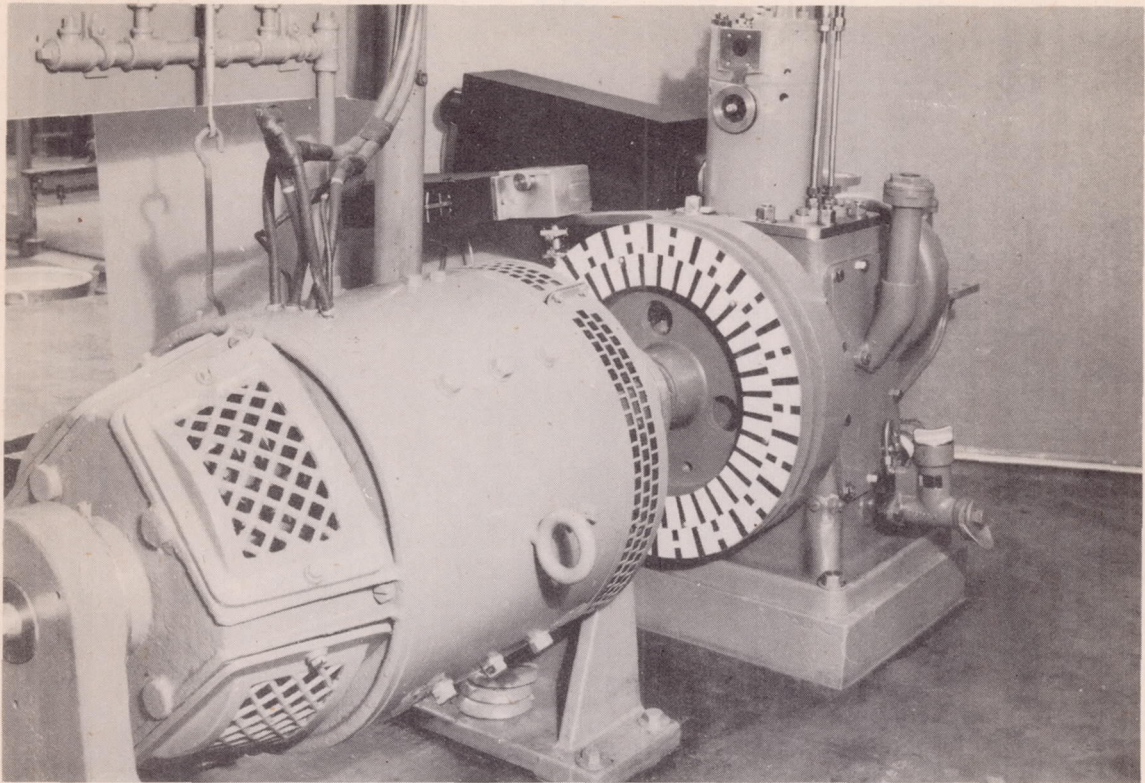


Figure 3.- Dynamometer end of friction engine.

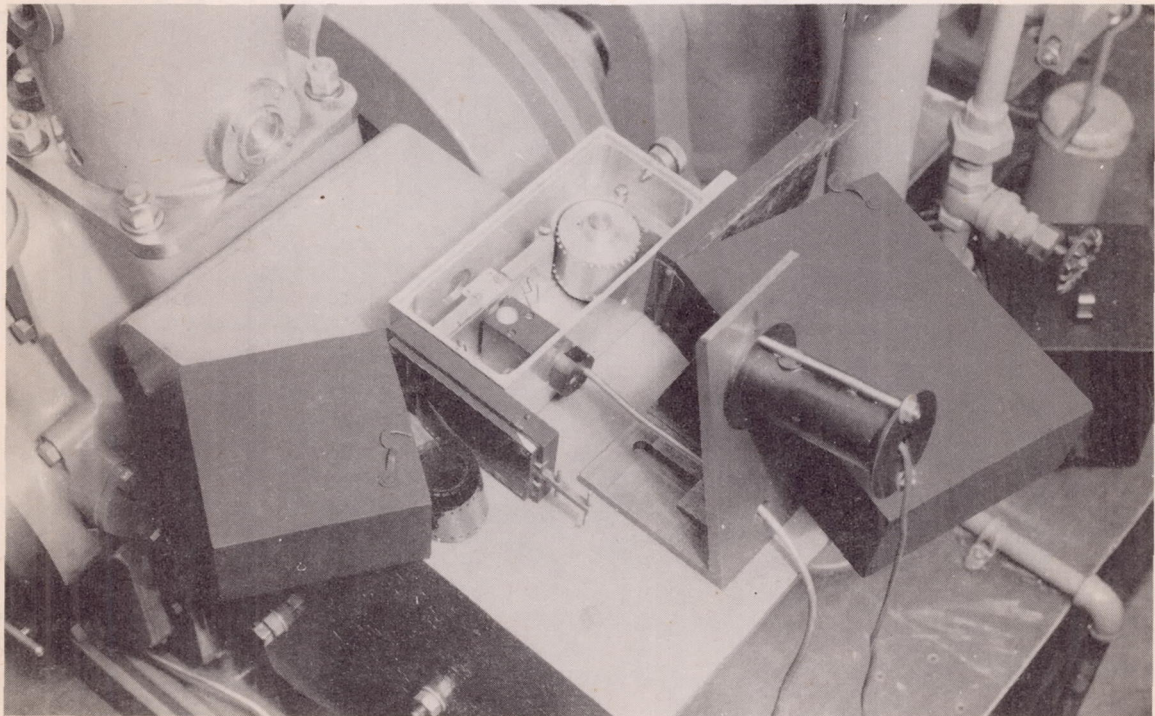


Figure 5.- Details of friction engine camera.

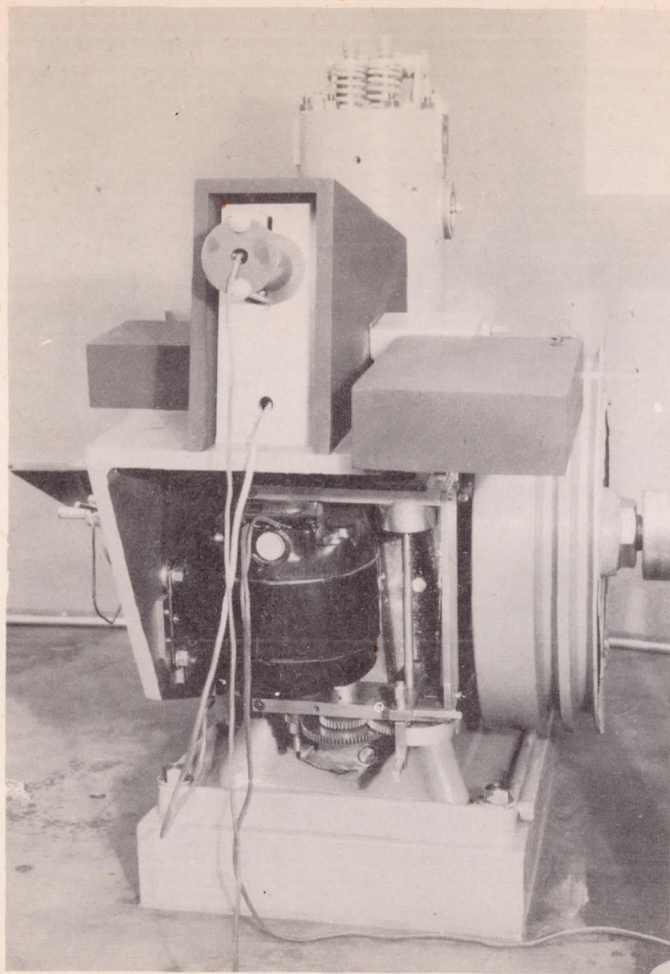
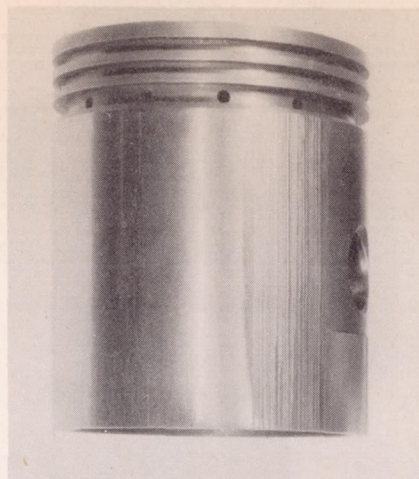
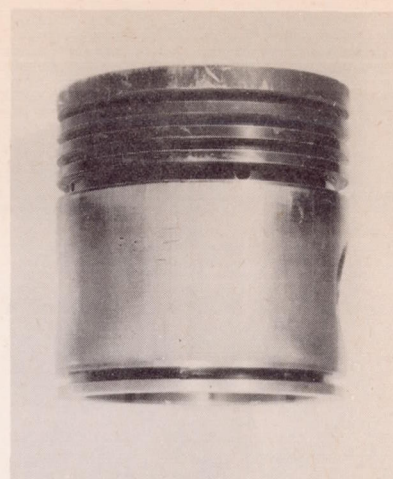


Figure 4.- Assembled camera motor,
camera, and light source.



(B) Cast iron



(A) Aluminum alloy

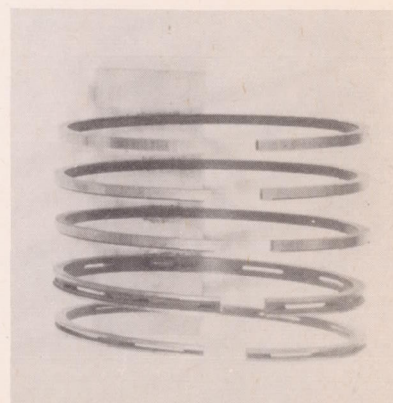
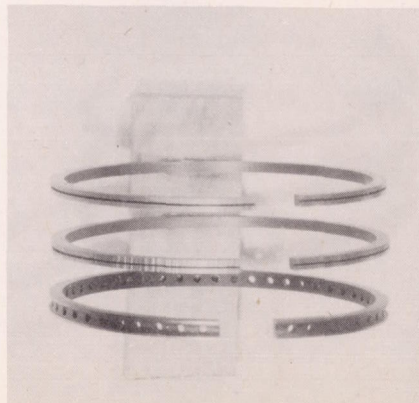


Figure 9.- Pistons used in friction
engine.

NACA

Figs. 4, 9

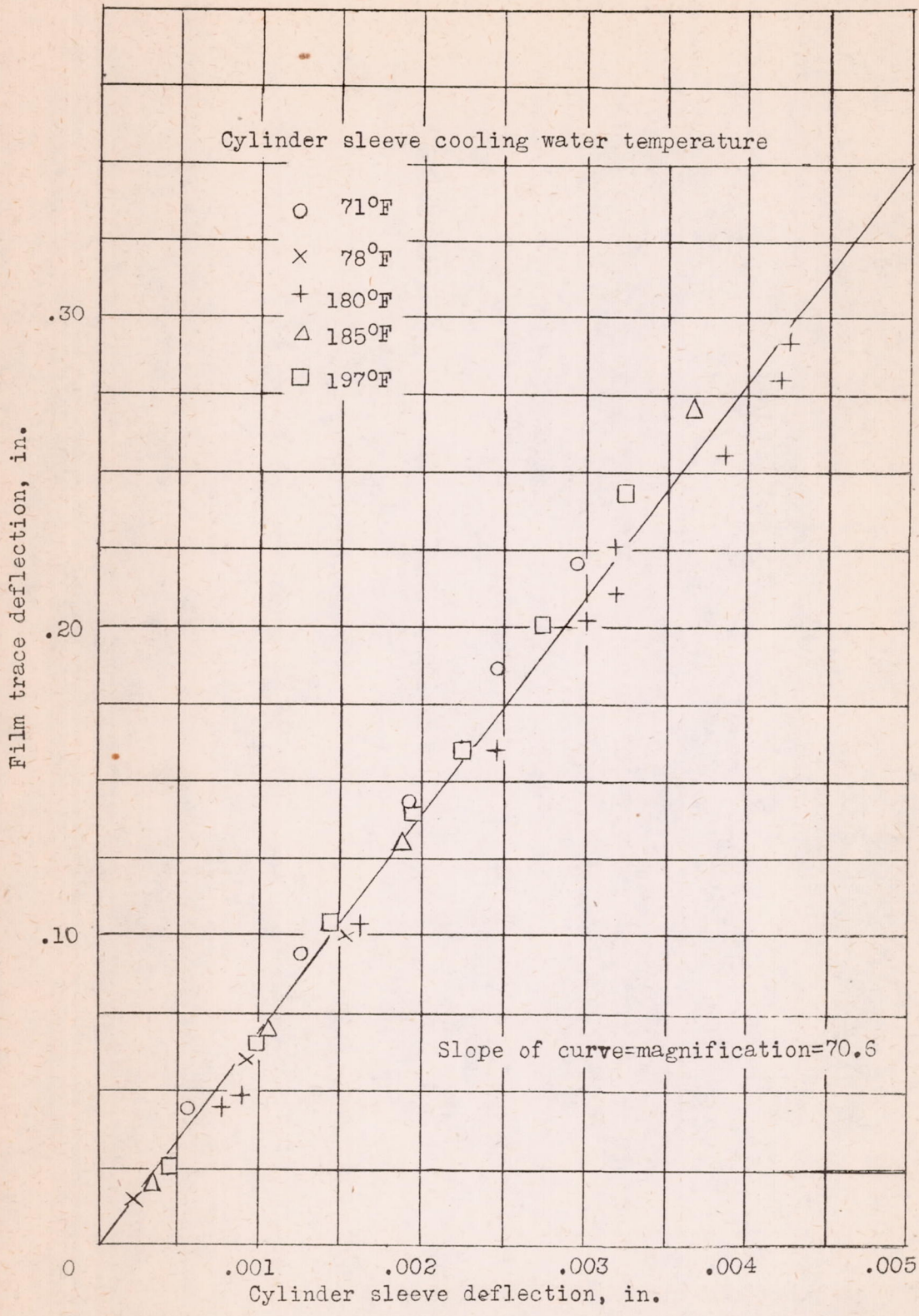


Figure 6.- Calibration of cylinder sleeve displacement recording mechanism.

W-37

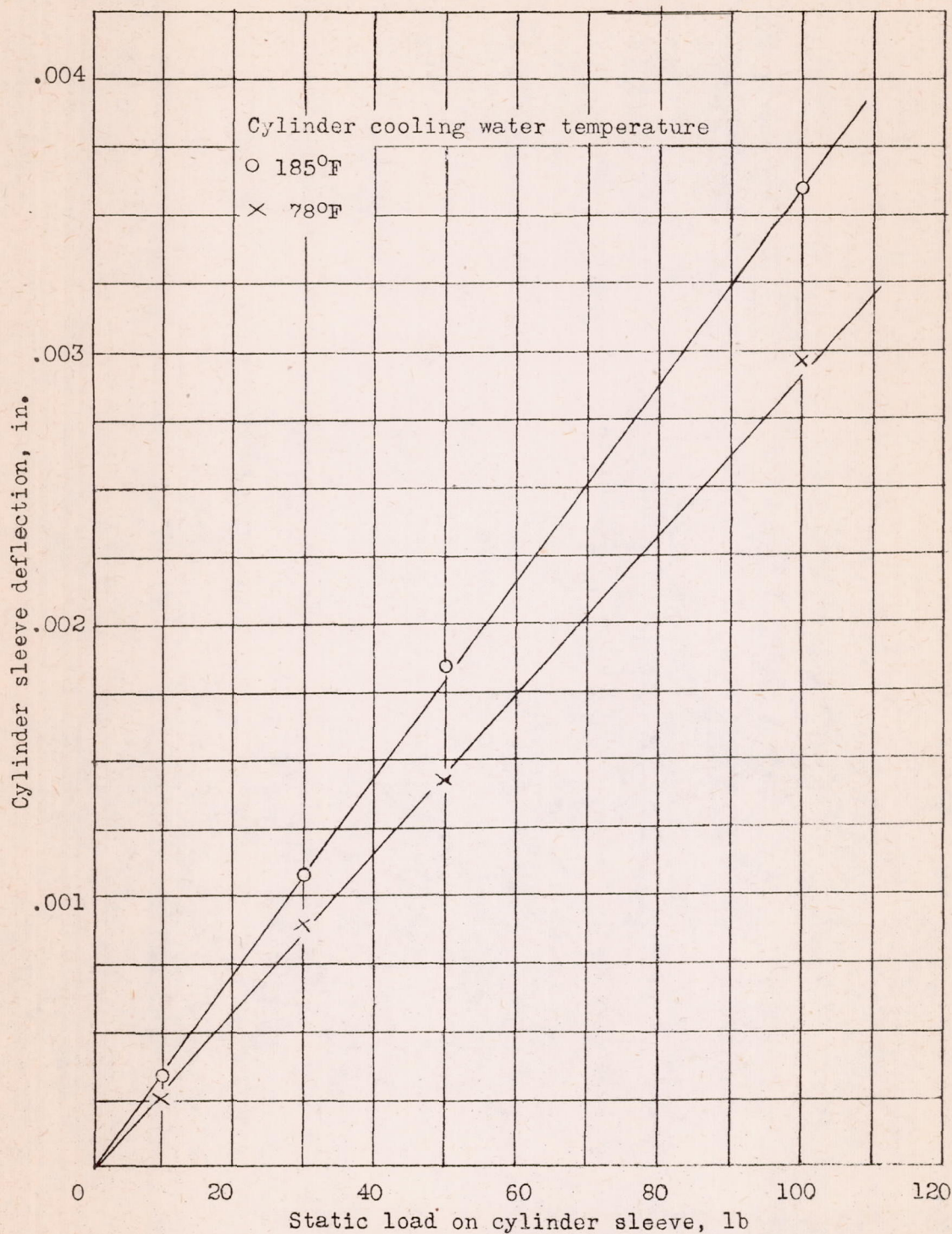


Figure 7.- Static load deflection of cylinder sleeve for two different cylinder sleeve cooling water temperatures.

W-37

W-37

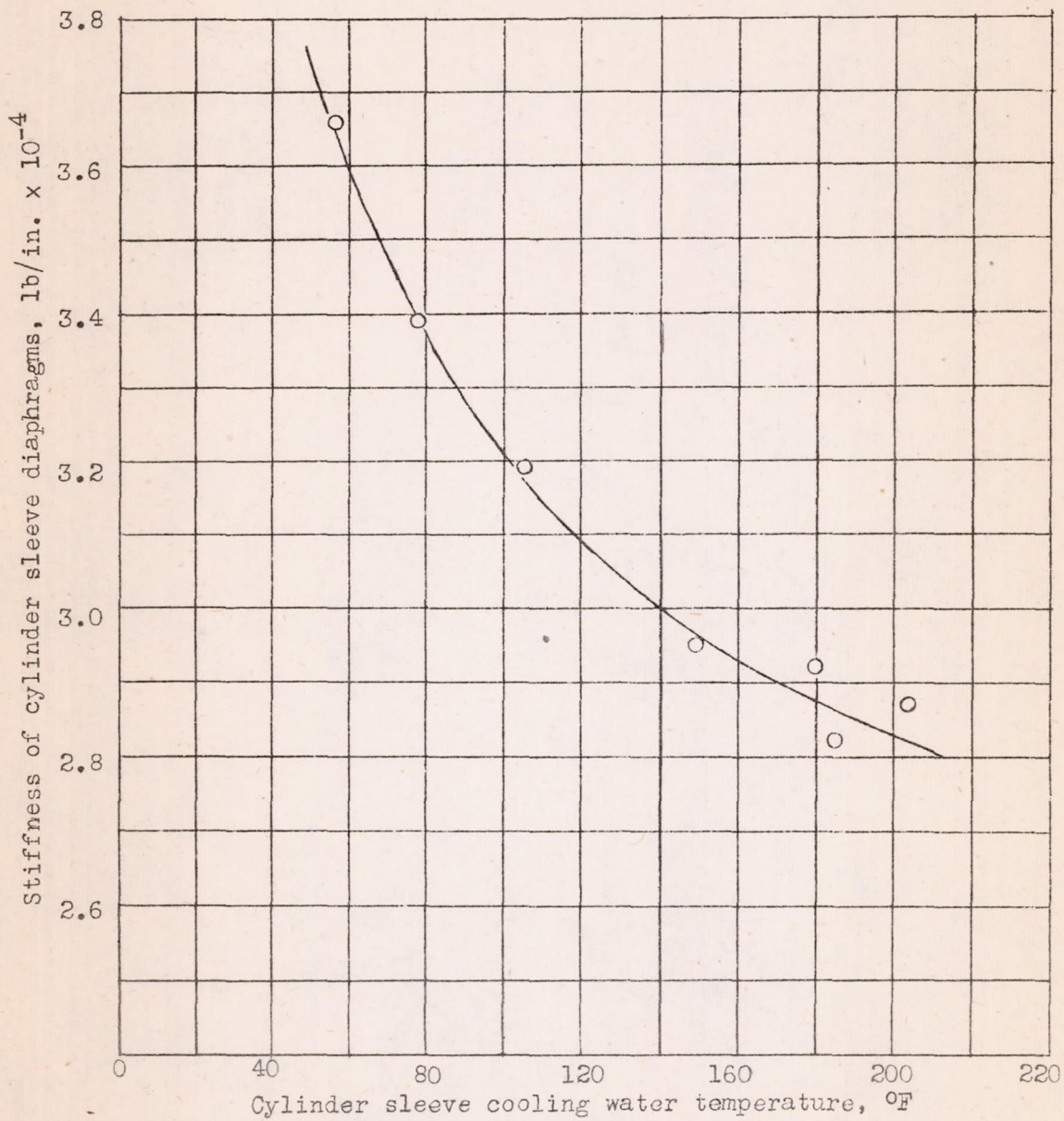
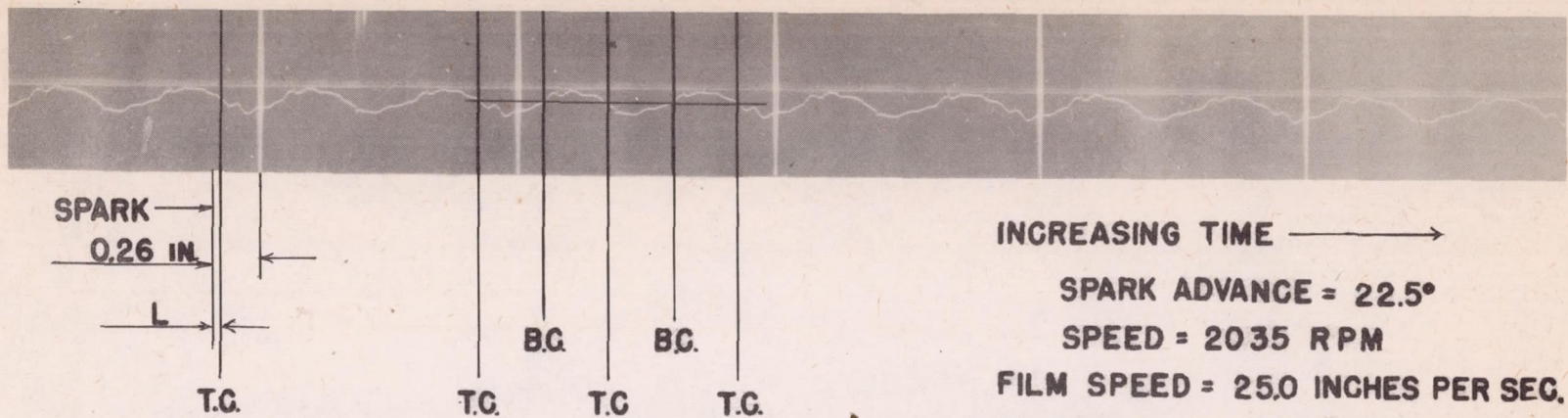
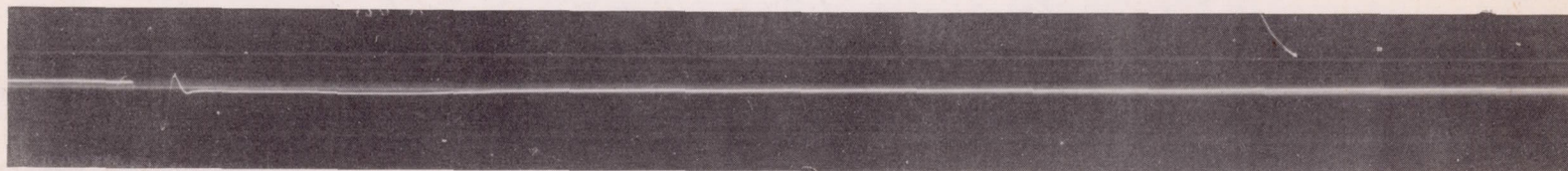


Figure 8.- Apparent stiffness of cylinder sleeve as a function of cylinder sleeve cooling water temperature.

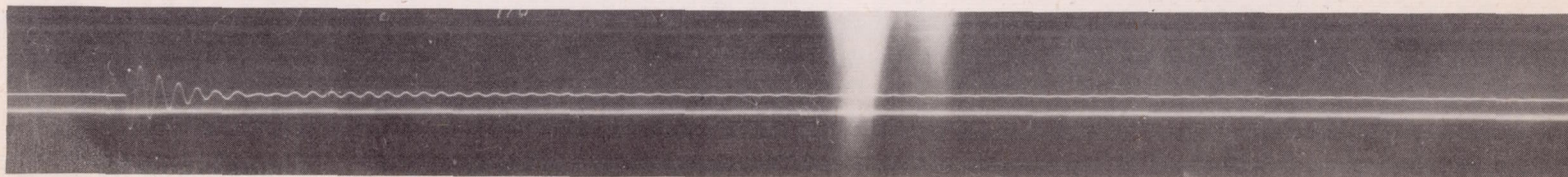


NACA

Figure 10.- Typical piston friction record for engine firing.



Assembled Engine



Dummy Cylinder Head -- No Piston

Figure 11.- Natural frequency of cylinder sleeve.

Figs. 10.11

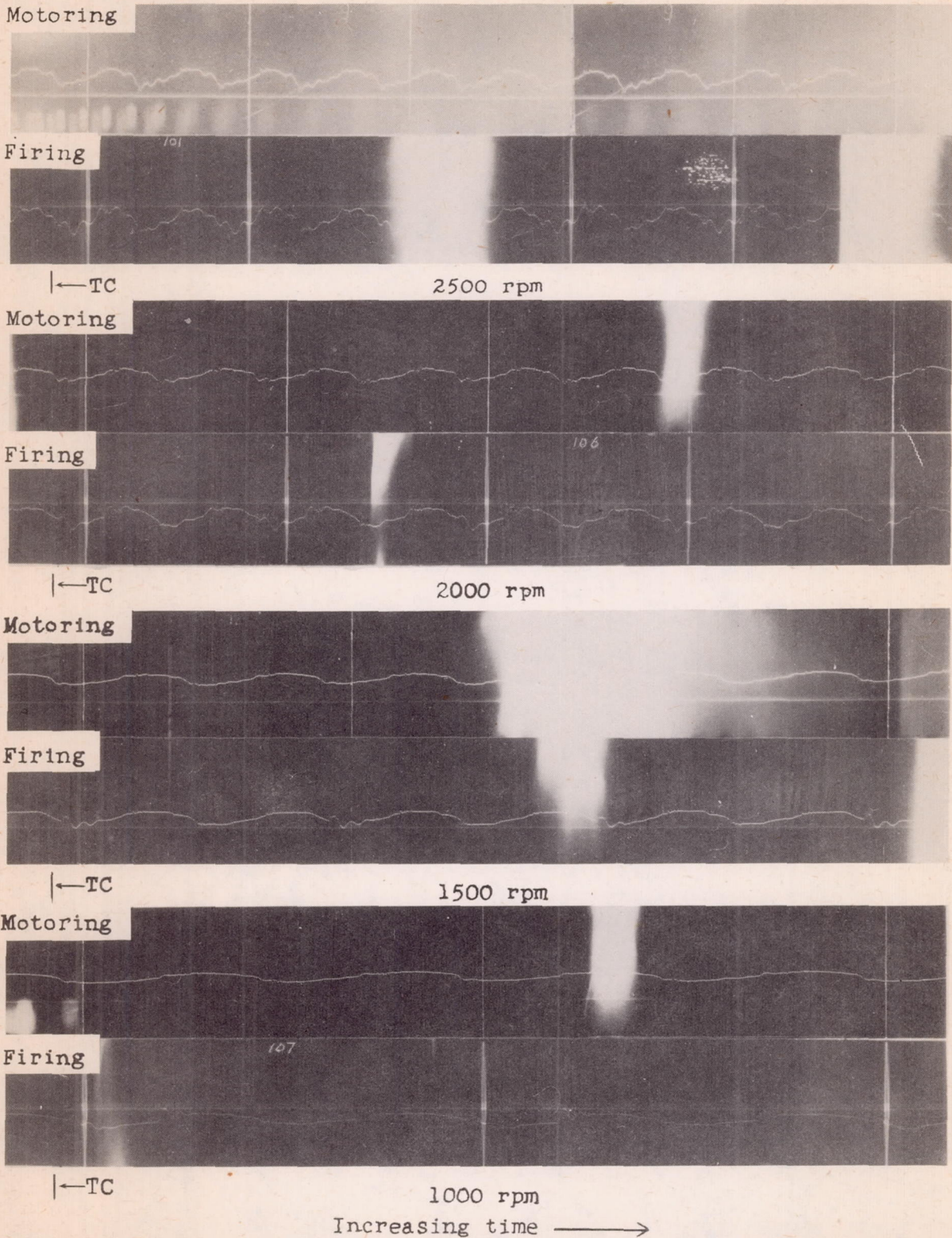
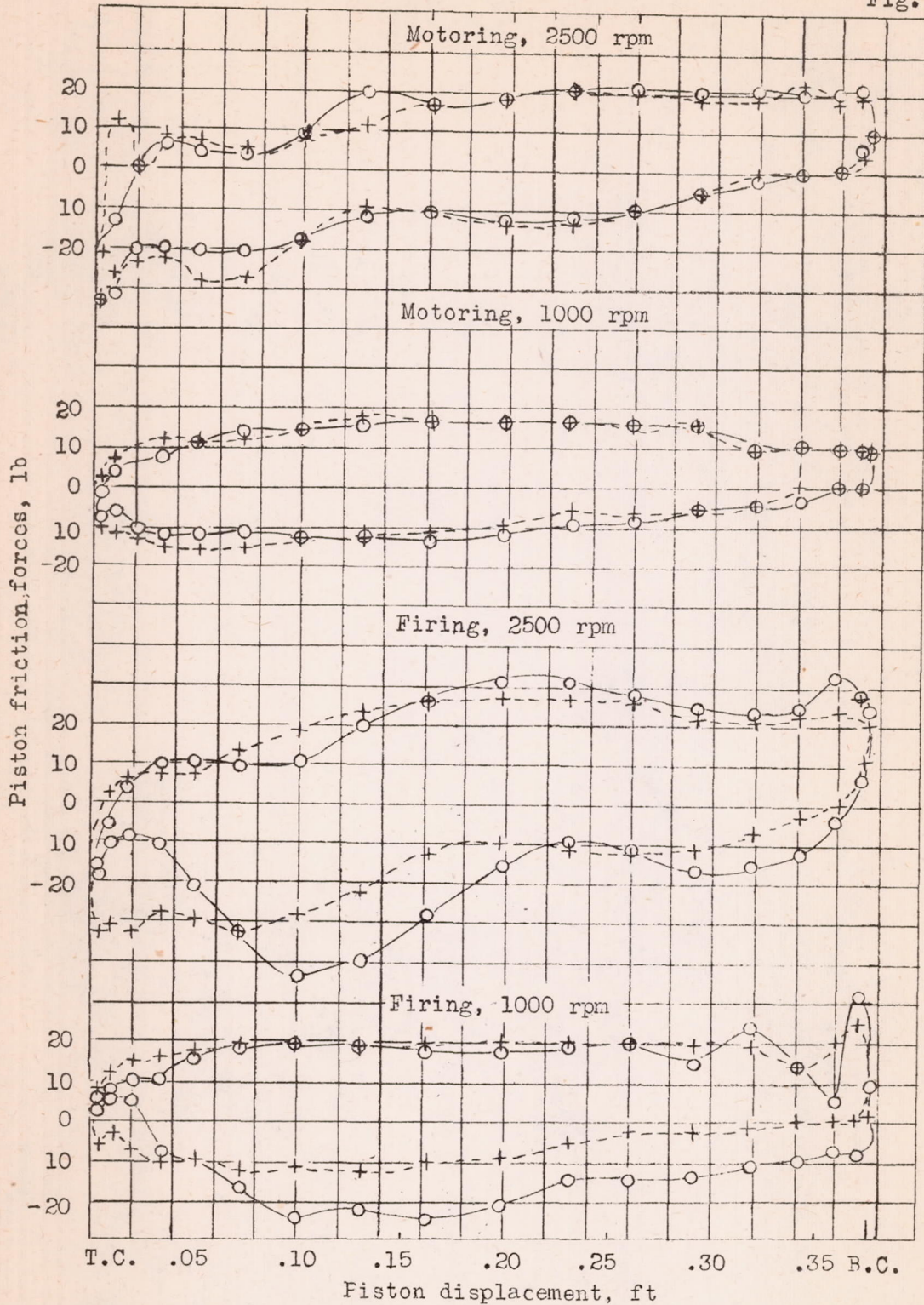


Figure 12.- Cylinder sleeve displacement as a function of speed. Oil and cylinder sleeve cooling water temperatures held constant at 180°F. SAE 40 oil.



W-37

Figure 13.- Piston friction force as a function of piston displacement for two speeds at full load. Positive forces correspond to up-stroke of piston. Full lines represent expansion-exhaust strokes. Oil and cylinder cooling water temperatures 180°F, SAE 40 oil.

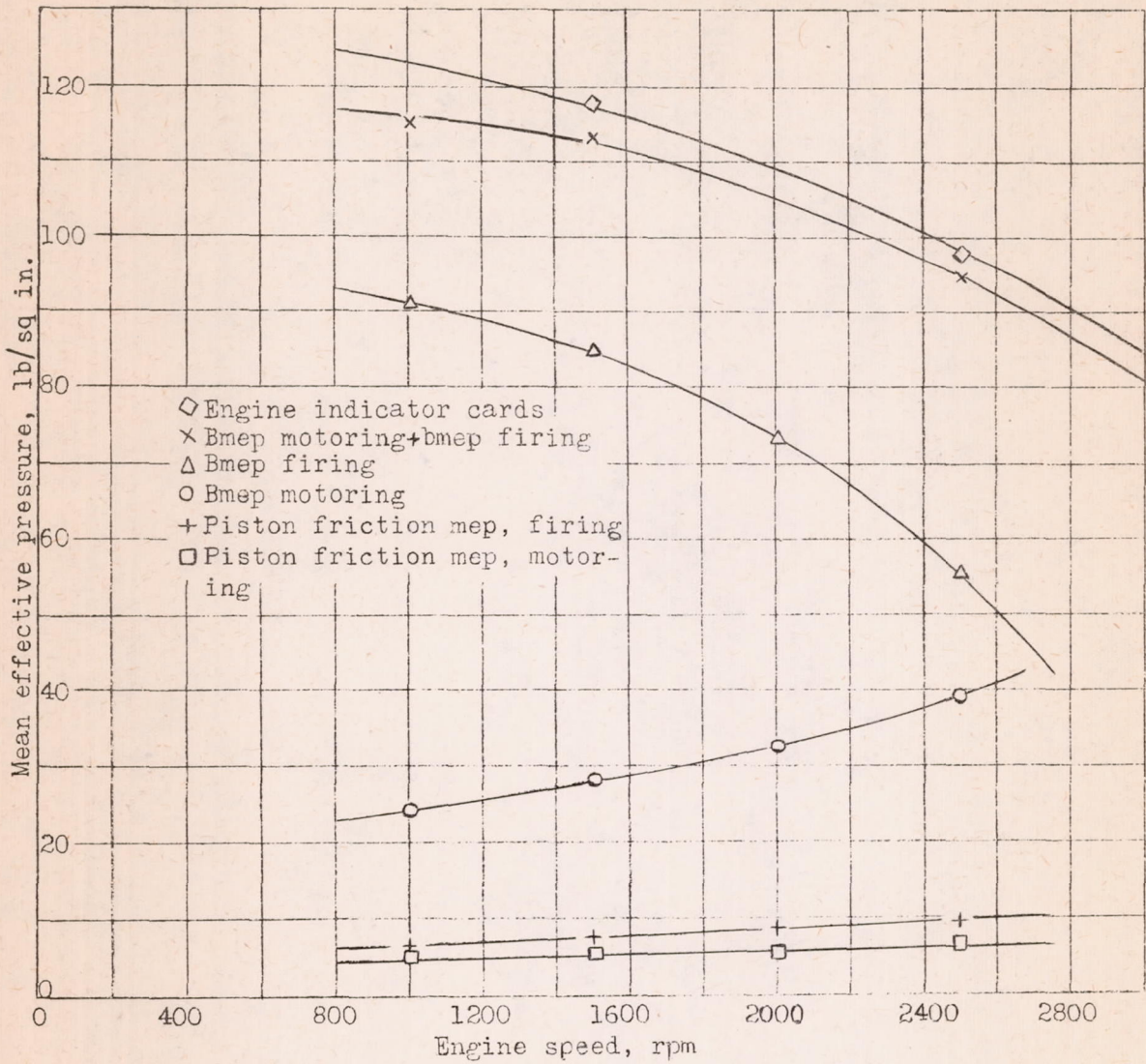


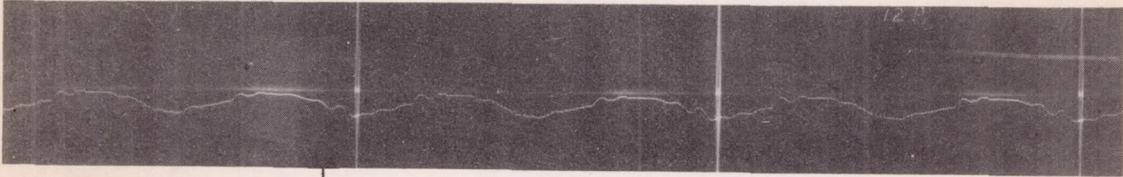
Figure 14.- Piston friction mean effective pressure as a function of engine speed at full load. Oil and cylinder cooling water temperatures 180°F. SAE 40 oil.

W-37

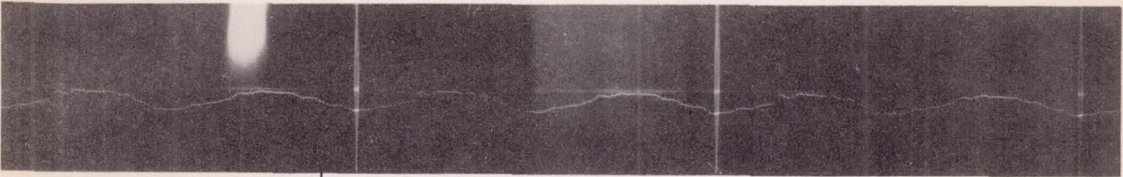
Full load



Half load

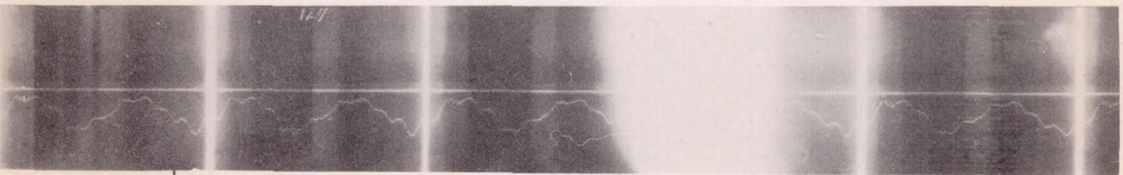


Idling



TC → 1500 rpm
Increasing time →

Full load



Half load



Idling



TC → 2500 rpm

Figure 15.- Cylinder sleeve displacement as a function of load. Oil and cylinder sleeve cooling water temperatures held constant at 180°F. SAE 40 oil.

W-37

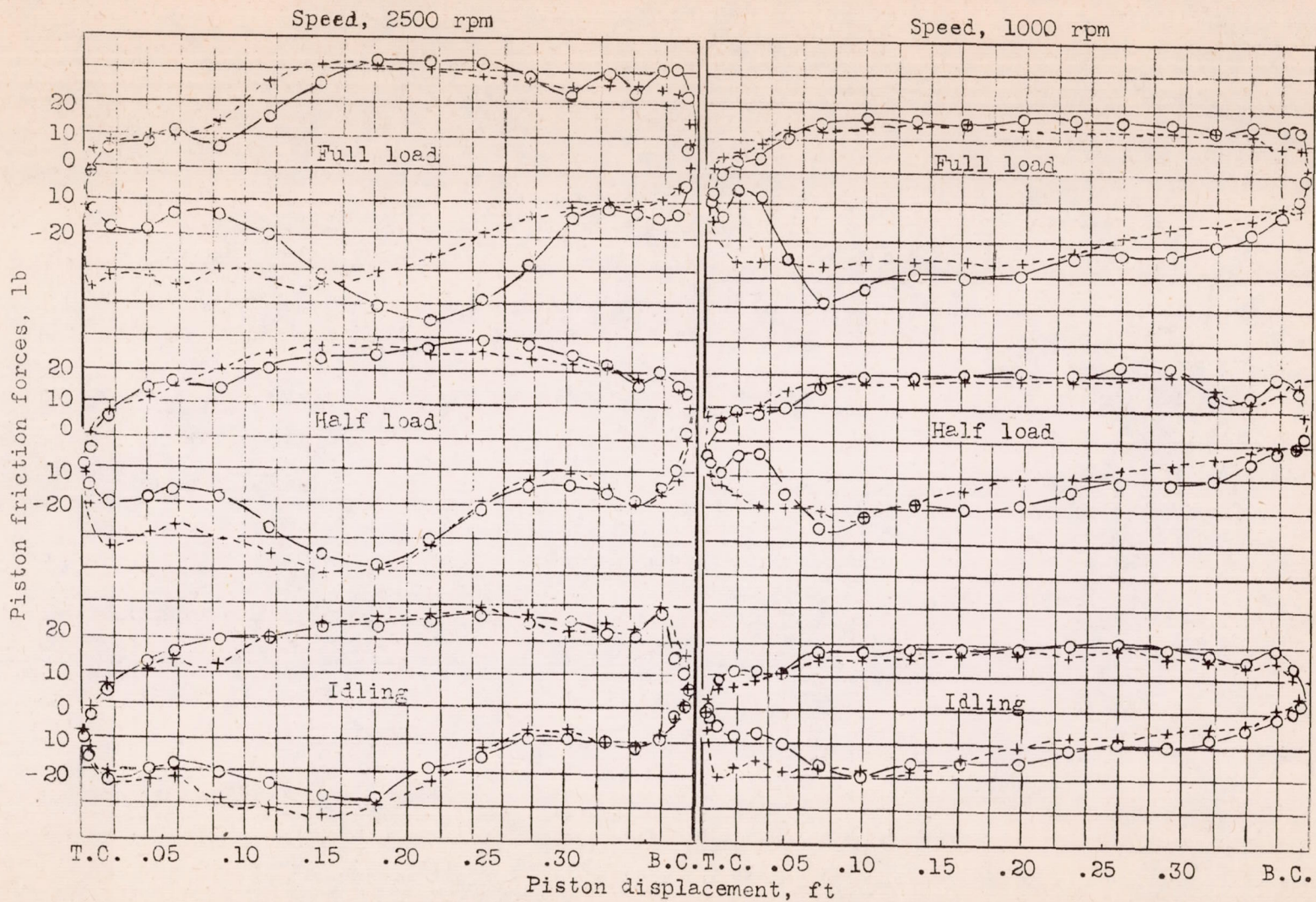


Figure 16.- Piston friction force as a function of piston displacement for three loads and two speeds. Notation same as in figure 13. Oil and cylinder cooling water temperatures 180°F. SAE 40 oil.

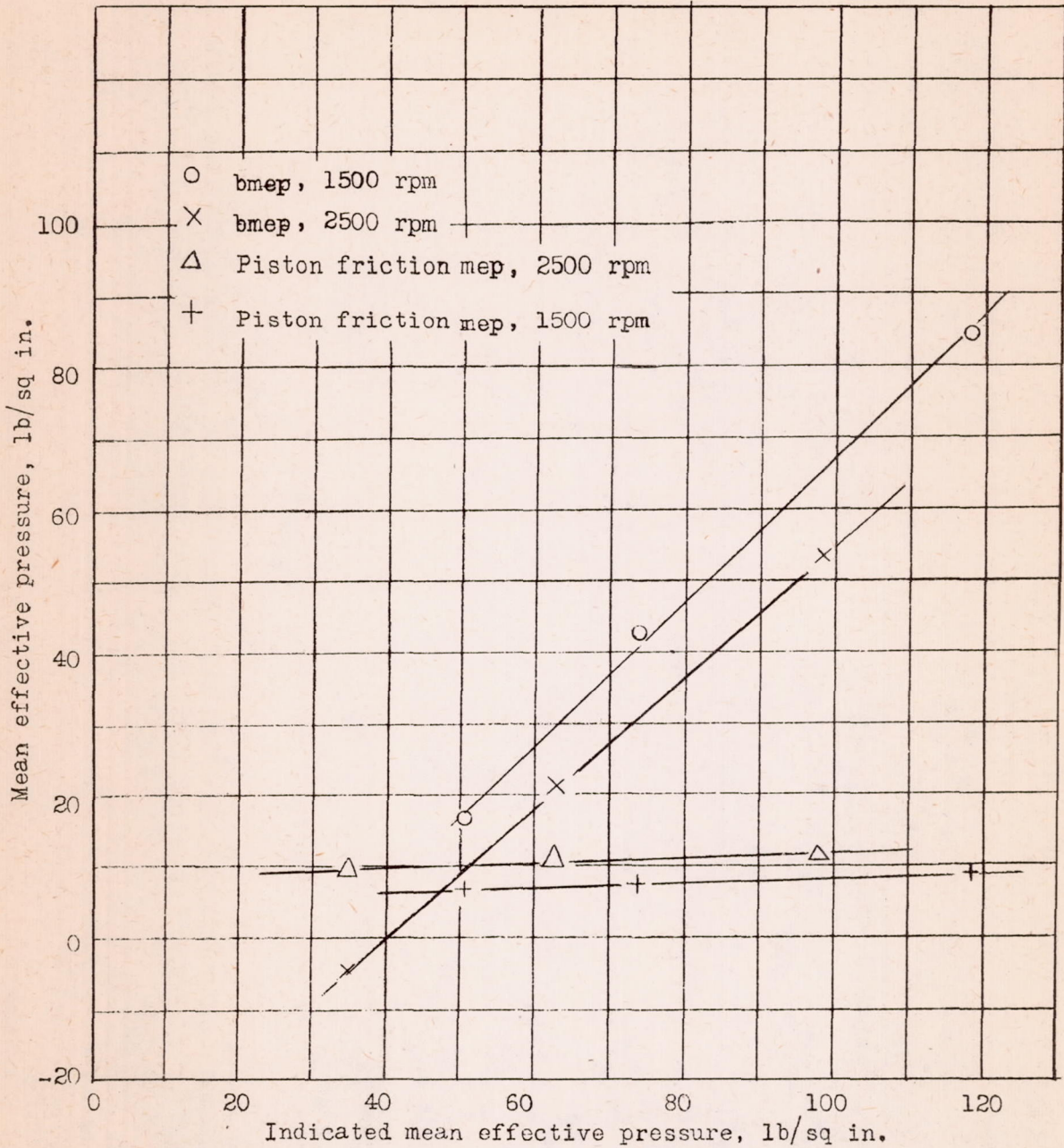


Figure 17.- Piston friction mean effective pressure as a function of indicated mean effective pressure for two engine speeds. Oil and cylinder cooling water temperatures 180°F, SAE 40 oil.

W-37

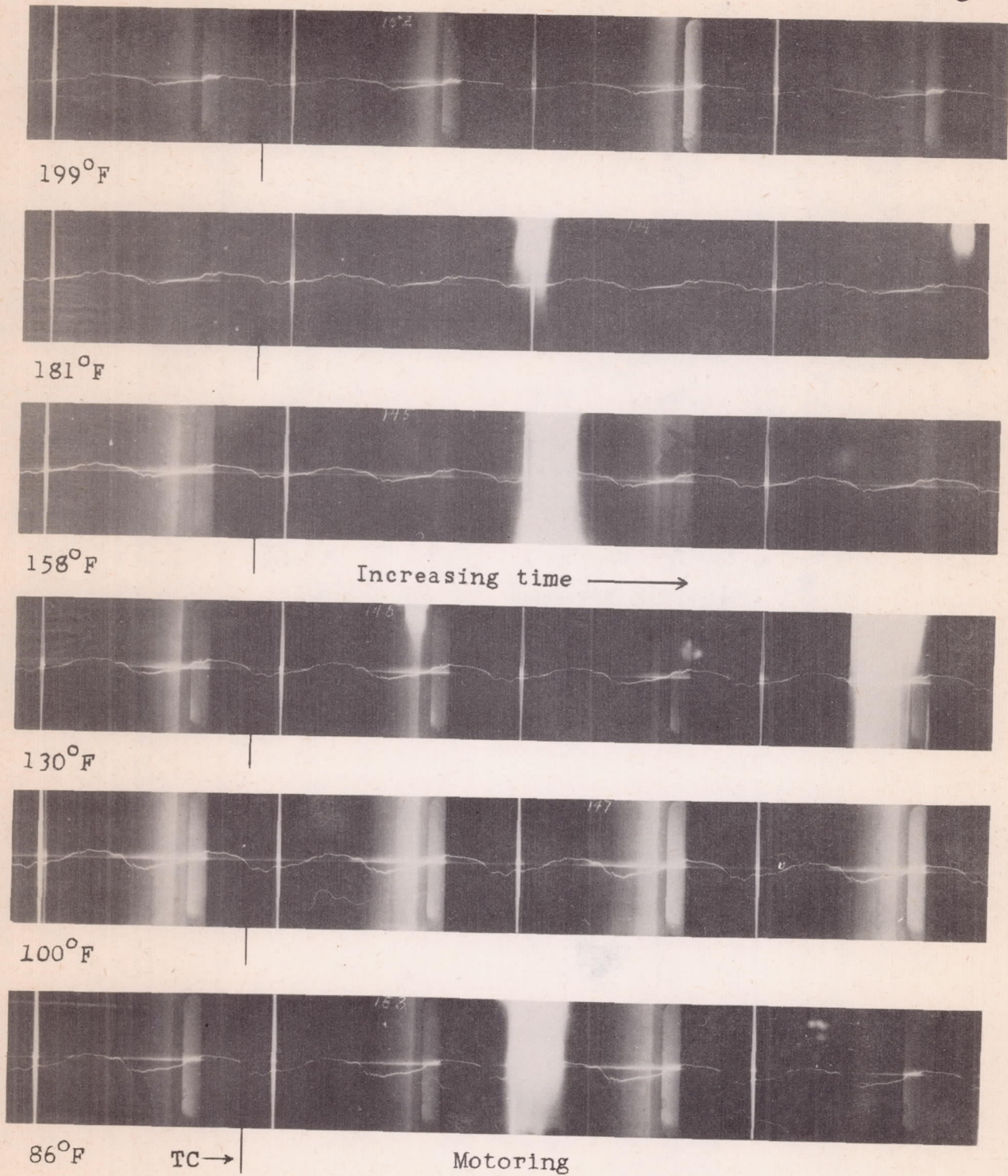


Figure 18a.- Cylinder sleeve displacement as a function of common oil and cylinder sleeve cooling water temperatures. SAE 20 oil. Speed 1800 rpm.

W-37

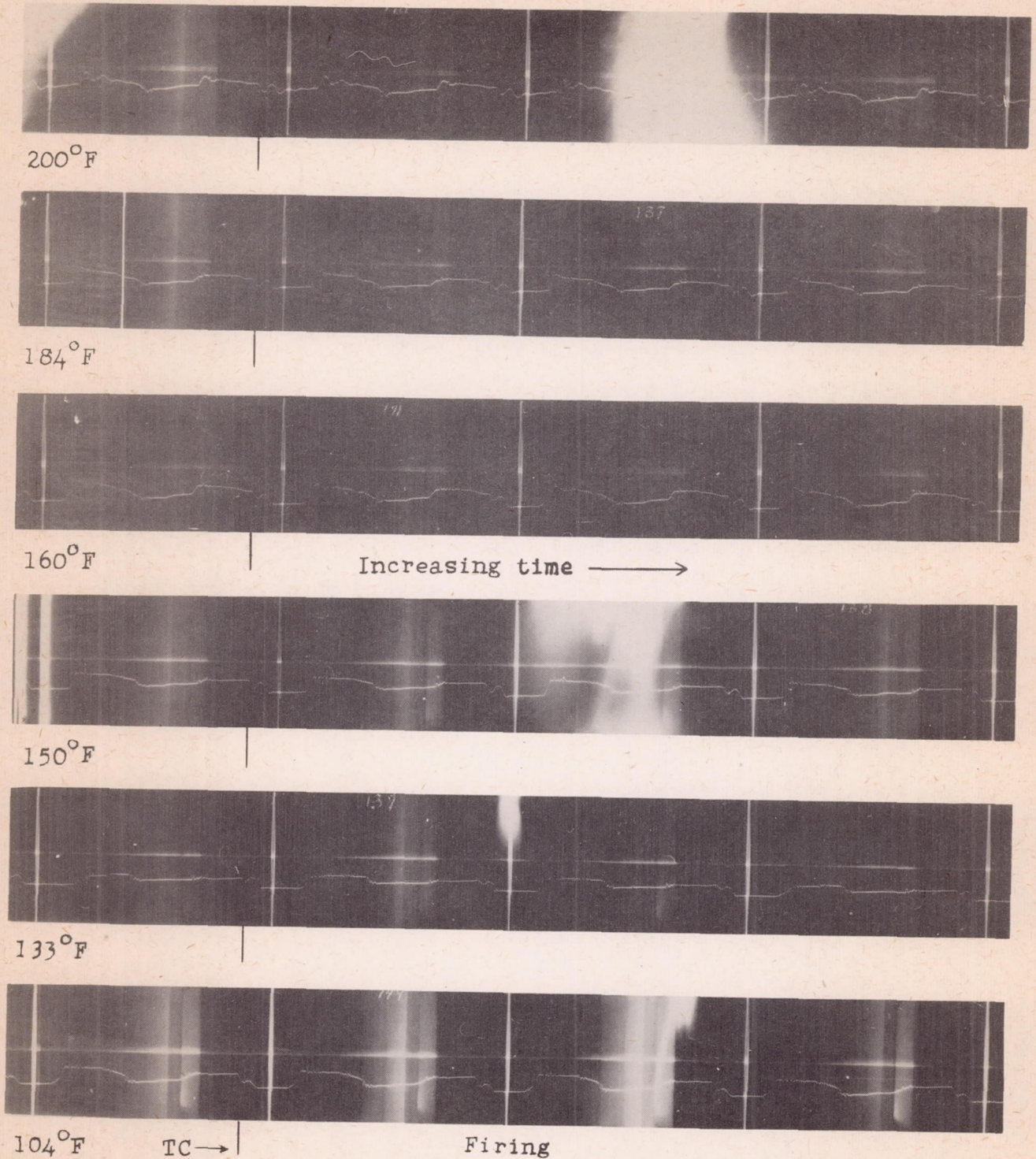


Figure 18b.- Cylinder sleeve displacement as a function of common oil and cylinder sleeve cooling water temperatures. SAE 20 oil. Speed 1800 rpm.

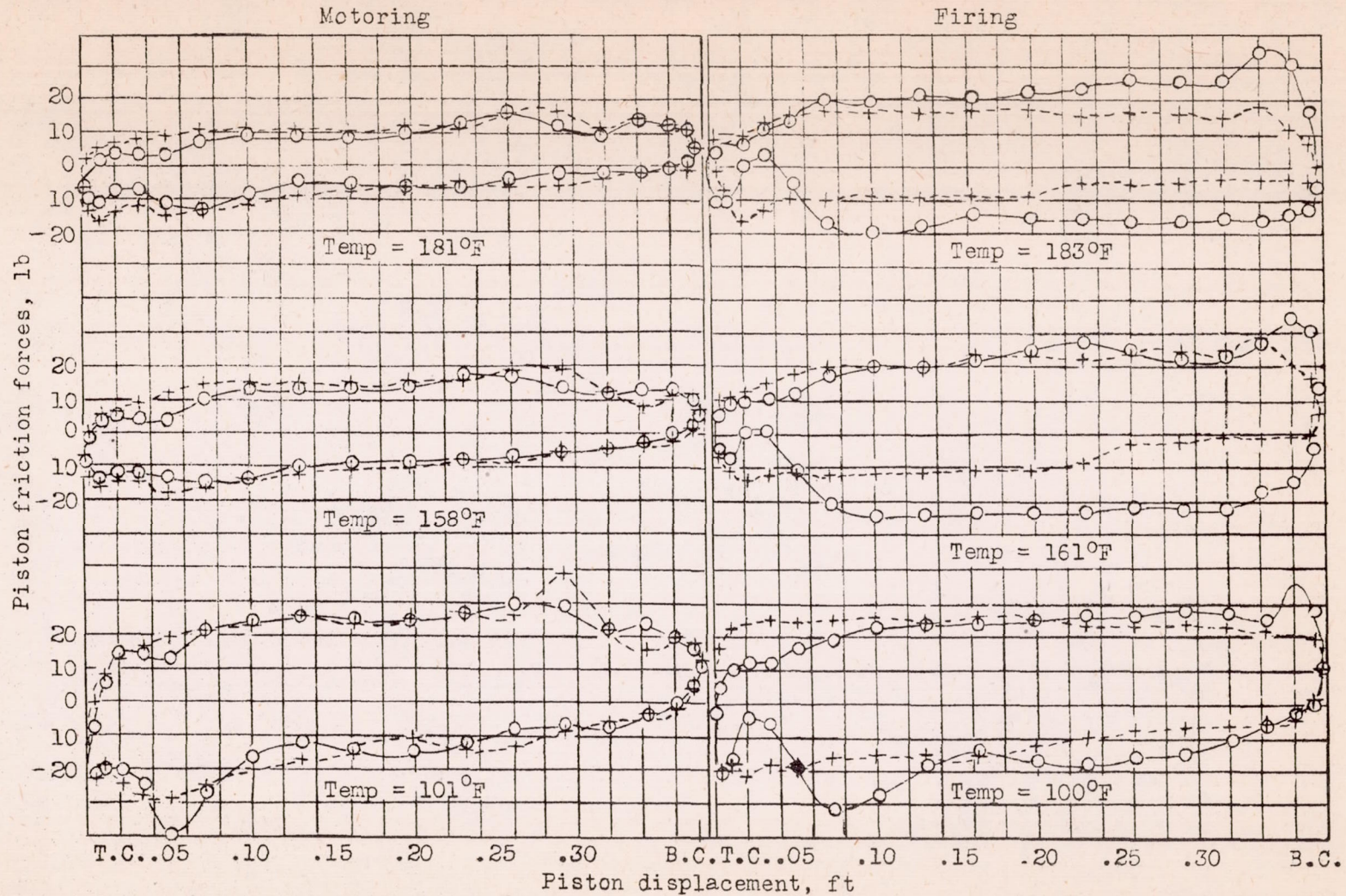


Figure 19.- Piston friction force as a function of piston displacement at a constant speed of 1800 rpm. Common oil and cylinder cooling water temperatures varied as indicated. SAE 20 oil. Notation same as in figure 13.

A SAE 40

B SAE 20

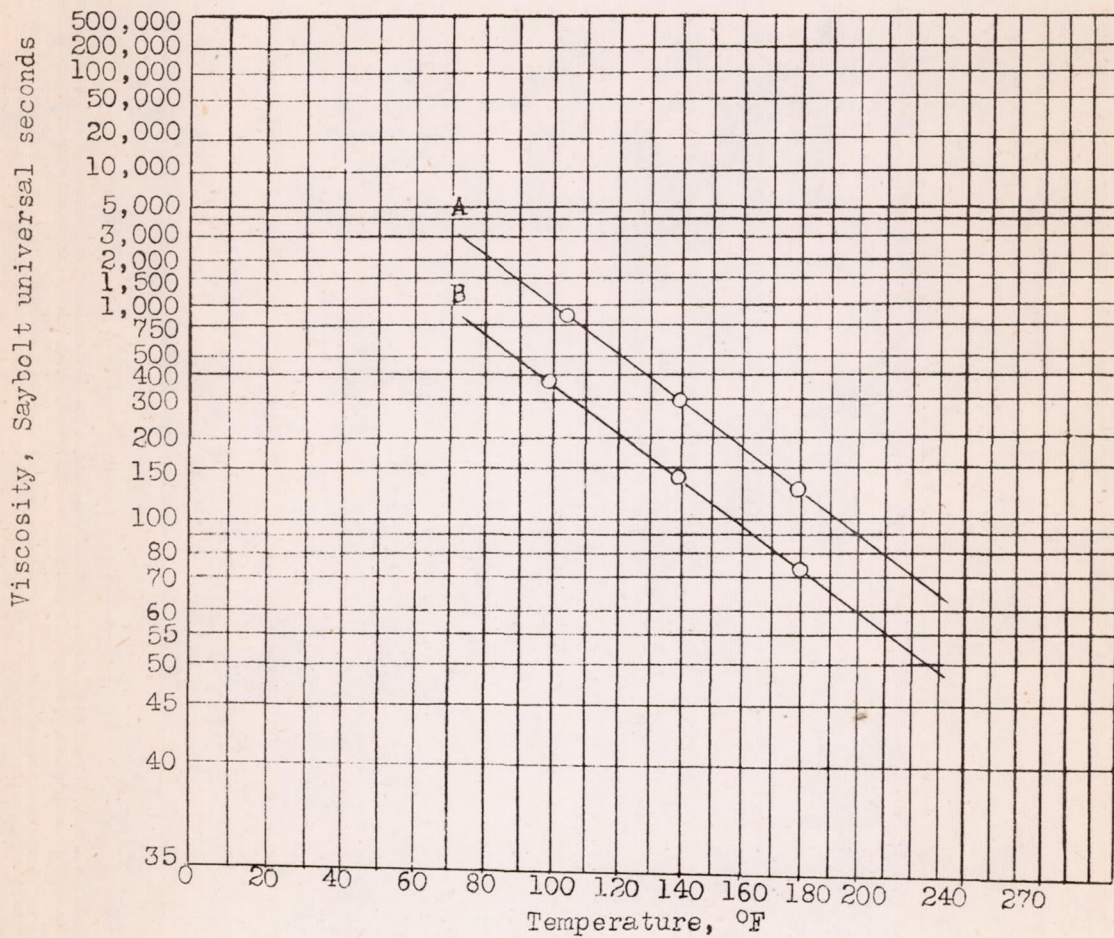


Figure 20.- Temperature variation of the Saybolt universal viscosities of the two oils used in the piston friction engine.

W-37

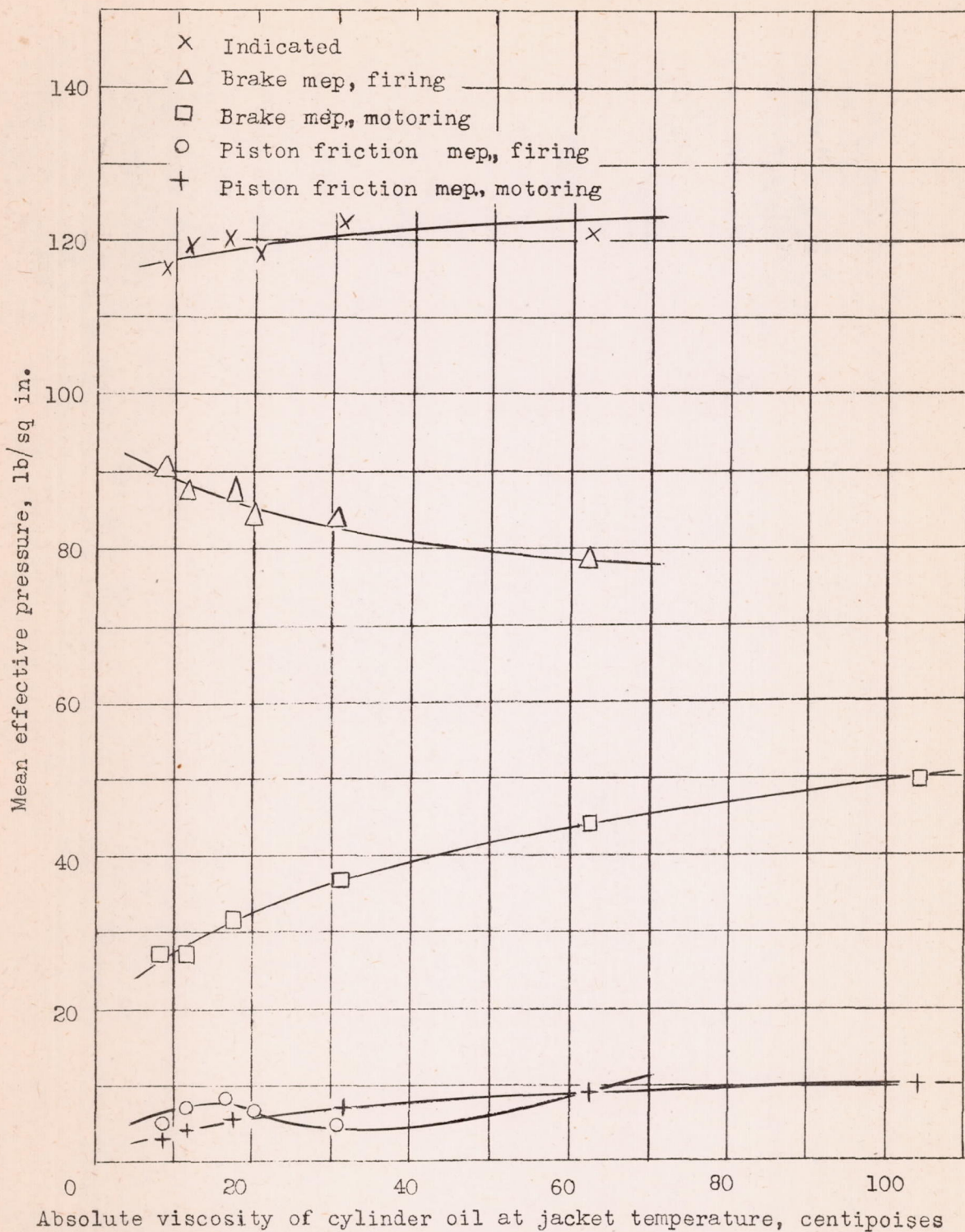


Figure 21.- Variation of piston friction mean effective pressure as a function of absolute viscosity. Engine speed 1800 rpm. SAE 20 oil.

W-37

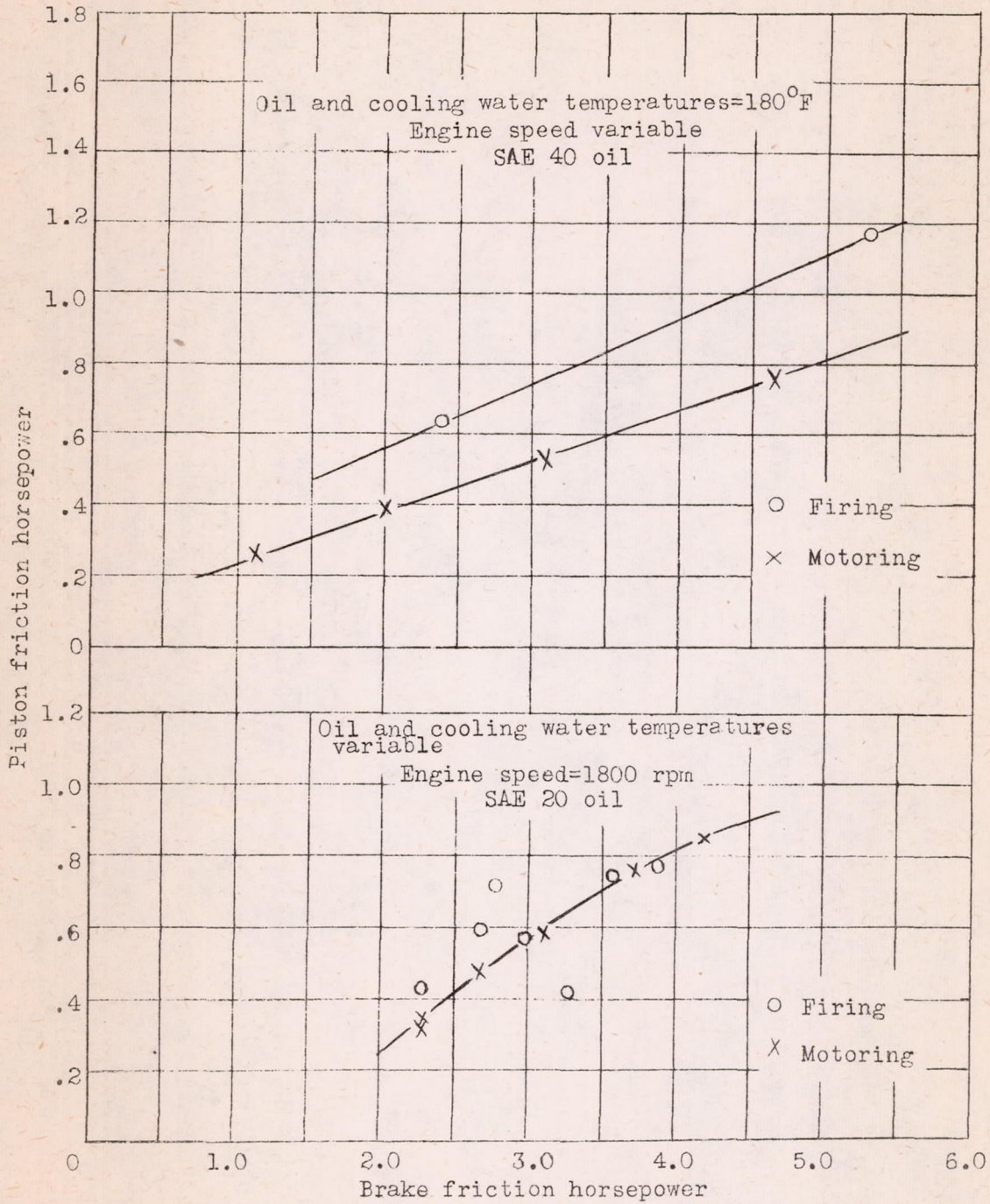


Figure 22.- Piston friction horsepower as a function of brake friction horsepower.

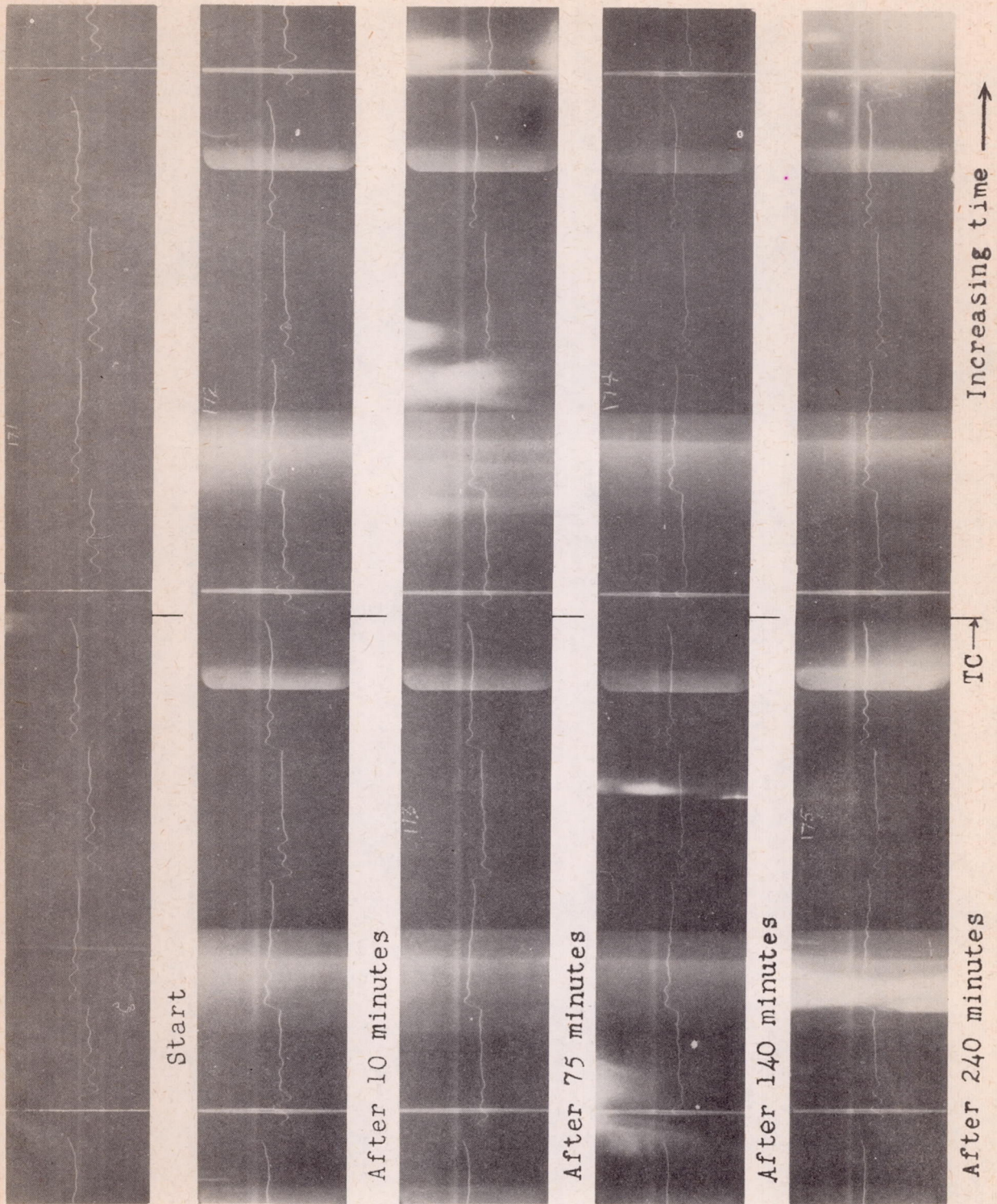


Figure 23.- Cylinder sleeve displacement as a function of time during the motoring "running in" of the cast iron piston. Speed 900 rpm. Temperatures of oil and cooling water 160°F. SAE 20 oil.

W-37